Three-group ROC analysis: A nonparametric predictive approach

Tahani Coolen-Maturi[a], Faiza F. Elkhafifi[b], Frank P.A. Coolen[c,*]

[a]*Durham University Business School, Durham University, Durham, DH1 3LB, UK*
[b]*Department of Statistics, Benghazi University, Benghazi, LIBYA*
[c]*Department of Mathematical Sciences, Durham University, Durham, DH1 3LE, UK*

Abstract

Measuring the accuracy of diagnostic tests is crucial in many application areas, in particular medicine and health care. The receiver operating characteristic (ROC) surface is a useful tool to assess the ability of a diagnostic test to discriminate among three ordered classes or groups. In this paper, nonparametric predictive inference (NPI) for three-group ROC analysis is presented. NPI is a frequentist statistical method that is explicitly aimed at using few modelling assumptions in addition to data, enabled through the use of lower and upper probabilities to quantify uncertainty. It focuses exclusively on a future observation, which may be particularly relevant if one considers decisions about a diagnostic test to be applied to a future patient. This paper presents the NPI approach to three-group ROC analysis, including results on the volumes under the ROC surfaces and choice of decision thresholds for the diagnosis.

Keywords: Diagnostic accuracy, Lower and upper probability, Nonparametric predictive inference, Receiver operating characteristic (ROC) surface, Youden's index.

*Corresponding author
Email addresses: tahani.maturi@durham.ac.uk (Tahani Coolen-Maturi), f_elkhafifi@yahoo.com (Faiza F. Elkhafifi), frank.coolen@durham.ac.uk (Frank P.A. Coolen)

1. Introduction

Measuring the accuracy of diagnostic tests is crucial in many application areas, in particular medicine and health care (Wians et al., 2001; Pepe, 2003; Xiong et al., 2007; Lopez-de Ullibarri et al., 2008; Tian et al., 2011; Rodriguez-Alvarez et al., 2011a,b; Chen et al., 2012), the same statistical methods are used in other fields such as credit scoring (Xanthopoulos and Nakas, 2007). Good methods for determining diagnostic accuracy provide useful guidance on selection of patient treatment according to the severity of their health status. The receiver operating characteristic (ROC) surface is a useful tool to assess the ability of a diagnostic test to discriminate among three ordered classes or groups. The construction of the ROC surface based on the probabilities of correct classification for three classes has been introduced by Mossman (1999), Nakas and Yiannoutsos (2004) and Nakas and Alonzo (2007). They also considered the volume under the ROC surface (VUS) and its relation to the probability of correctly ordered observations from the three groups. The three-group ROC surface generalizes the popular two-group ROC curve, which in recent years has attracted much theoretical attention and has been widely applied for analysis of accuracy of diagnostic tests (Zhou et al., 2011; Zou et al., 2011).

Statistical inference for accuracy of diagnostic tests using ROC curves or surfaces has mostly focused on estimating the relevant probabilities of correct classification for the different groups, with these probabilities being considered as properties of assumed underlying populations. While this is a well-established approach, with methods presented for fully parametric models as well as semiparametric and nonparametric methods (Heckerling, 2001; Li and Zhou, 2009), the practical importance of diagnostic tests is in their use for future patients. As such, it is of interest to study a predictive statistical approach to such inferences on accuracy of diagnostic tests. The importance of prediction is well understood, e.g. Airola et al. (2011) and van Calster et al. (2012) explicitly mention 'predictive models' and 'prediction models', but thus far the statistical approaches used in this field have mostly been based on estimation, with their predictive performance investigated via numerical studies.

Nonparametric predictive inference (NPI) is a frequentist method using few modelling assumptions, and hence is strongly data-driven, which is enabled by the use of lower and upper probabilities to quantify uncertainty (Augustin and Coolen, 2004; Coolen, 2006, 2011). Lower and upper proba-

bilities generalize the classical theory of (precise) probability (Coolen et al., 2011), with the difference between the upper and lower probabilities for an event typically reflecting the amount of information available. In NPI, the lower and upper probabilities always provide bounds for empirical probabilities, hence the NPI-based statistical conclusions are never contradictory to those based on empirical probabilities (Coolen, 2006). Due to the importance of prediction of the accuracy of diagnostic tests for a future patient, NPI provides an attractive alternative approach to the established methods in this field. NPI has recently been introduced for assessing the accuracy of a classifier's ability to discriminate between two groups for binary data (Coolen-Maturi et al., 2012a), ordinal data (Elkhafifi and Coolen, 2012) and real-valued data (Coolen-Maturi et al., 2012b).

This paper introduces NPI for three-group ROC analysis for real-valued data. Section 2 presents an introduction to three-group ROC analysis, followed in Section 3 by a brief introduction to NPI. NPI for three-group ROC analysis is presented in Section 4 and illustrated by an example in Section 5. The paper ends with concluding remarks in Section 6 and two appendices containing proofs.

2. Three-group ROC analysis

In this section we introduce the concepts and notation of three-group ROC analysis (Mossman, 1999; Nakas and Yiannoutsos, 2004; Nakas and Alonzo, 2007). Consider three groups, denoted by G_x, G_y and G_z. Throughout this paper, we assume that these groups are fully independent, in the sense that any information about one of the groups does not hold any information about another group. Let real-valued observed test results be denoted by $x_1, x_2, ..., x_{n_x}$ for group G_x, $y_1, y_2, ..., y_{n_y}$ for group G_y and $z_1, z_2, ..., z_{n_z}$ for group G_z. Suppose that a diagnostic test is used to discriminate the subjects from these groups. We assume that the three groups are ordered in the sense that observations from group G_x tend to be lower than those from group G_y, which in turn tend to be lower than those from group G_z. There will typically be overlap of observations from different groups, but the practical diagnostic setting is assumed to be such that observations from the three groups tend to be ordered in this way. The cumulative distribution function (CDF) for the test outcomes of group $G_\cdot$ is denoted by $F_\cdot$.

Two decision thresholds $c_1 < c_2$ are required to classify a subject into one of the three groups, using the following rule, with T_j the test result

for subject j: Subject j is classified into group G_x if $T_j \leq c_1$, group G_y if $c_1 < T_j \leq c_2$ and group G_z if $T_j > c_2$. The test data are assumed to consist of measurements for individuals known to belong to specific groups, while the goal of the inferences is to develop a diagnostic classification method for individuals for who the group is unknown. We assume throughout the paper that the test data do not contain errors.

Denoting the classification measurement random quantity for a subject from group G_x, G_y, G_z by X, Y, Z, respectively, the corresponding probabilities of correct classification with thresholds (c_1, c_2) are $p_1 = P(X \leq c_1) = F_x(c_1)$, $p_2 = P(c_1 < Y \leq c_2) = F_y(c_2) - F_y(c_1)$ and $p_3 = P(Z > c_2) = 1 - F_z(c_2)$. The ROC surface, denoted by ROC_s, is constructed by plotting the triples (p_1, p_2, p_3) for all real-valued $c_1 < c_2$. A convenient way to define this ROC surface is as follows, for $p_1, p_3 \in [0, 1]$ (Inacio et al., 2011; Nakas and Yiannoutsos, 2004; Tian et al., 2011),

$$ROC_s(p_1, p_3) = \begin{cases} F_y(F_z^{-1}(1-p_3)) - F_y(F_x^{-1}(p_1)) & \text{if } F_x^{-1}(p_1) \leq F_z^{-1}(1-p_3) \\ 0 & \text{otherwise} \end{cases} \tag{1}$$

where $F_\cdot^{-1}(p)$ is the inverse function of the CDF $F_\cdot$.

The empirical estimator of the ROC surface can be obtained by replacing the CDFs in (1) with their empirical counterparts (Beck, 2005; Inacio et al., 2011), so for $p_1, p_3 \in [0, 1]$,

$$\widehat{ROC}_s(p_1, p_3) = \begin{cases} \hat{F}_y(\hat{F}_z^{-1}(1-p_3)) - \hat{F}_y(\hat{F}_x^{-1}(p_1)) & \text{if } \hat{F}_x^{-1}(p_1) \leq \hat{F}_z^{-1}(1-p_3) \\ 0 & \text{otherwise} \end{cases} \tag{2}$$

where $\hat{F}_x^{-1}(p) = x_i$ if $p \in (\frac{i-1}{n_x}, \frac{i}{n_x}]$, $i = 1, \ldots, n_x$, and $\hat{F}_x^{-1}(p) = -\infty$ if $p = 0$, with $\hat{F}_z^{-1}(p)$ defined similarly.

The volume under the ROC surface (VUS) is a global measure of the test's ability to discriminate between the three groups. The VUS is equal to the probability that three independent randomly selected measurements, one from each group, are correctly ordered, so that the observation from G_x is less than the observation from G_y and the latter is less than the observation from G_z (Mossman, 1999; Nakas and Yiannoutsos, 2010). An unbiased nonparametric estimator of the VUS is given by (Nakas and Yiannoutsos, 2004, 2010)

$$\widehat{VUS} = \frac{1}{n_x n_y n_z} \sum_{i=1}^{n_x} \sum_{j=1}^{n_y} \sum_{l=1}^{n_z} I(x_i < y_j < z_l) \tag{3}$$

with $I(A)$ equal to 1 if A is true and 0 else. Equation (3) gives the proportion of all possible triple combinations from the data that are correctly ordered, it is the empirical probability for this event based on the information from the data. It is (about) equal to 1/6 if the diagnostic test outcomes for the three groups completely overlap, in which case the data suggest that the test is not useful for the diagnosis. Perfect separation of the test results for the three groups, that is $x_i < y_j < z_l$ for all i,j and l, leads to $\widehat{VUS} = 1$. In practice, ties between measurements may occur, in this case a modified version of (3) should be used (Nakas and Yiannoutsos, 2004, 2010). In this paper, for ease of presentation we assume that no ties occur in the data.

Several approaches for choosing the thresholds c_1 and c_2 have been proposed in the literature (Greiner et al., 2000; Schafer, 1989; Yousef et al., 2009; Lai et al., 2012). We consider maximisation of Youden's index (Youden, 1950), which for three-group diagnostic tests was introduced by Nakas et al. (2010),

$$\begin{aligned} J(c_1, c_2) &= P(X \leq c_1) + P(c_1 < Y \leq c_2) - P(Z \leq c_2) + 1 \\ &= F_x(c_1) + F_y(c_2) - F_y(c_1) - F_z(c_2) + 1 \end{aligned} \tag{4}$$

$J(c_1, c_2)$ is equal to 1 if F_x, F_y and F_z are identical, perfect separation of the groups, $P(X < Y < Z) = 1$, leads to $J(c_1, c_2) = 3$.

3. Nonparametric predictive inference

Nonparametric predictive inference (NPI) (Augustin and Coolen, 2004; Coolen, 2006, 2011) is based on the assumption $A_{(n)}$ proposed by Hill (1968). Let $X_1, \ldots, X_n, X_{n+1}$ be real-valued absolutely continuous and exchangeable random quantities. Let the ordered observed values of $X_1, X_2, \ldots, X_n$ be denoted by $x_1 < x_2 < \ldots < x_n$ and let $x_0 = -\infty$ and $x_{n+1} = \infty$ for ease of notation. We assume that no ties occur; ties can be dealt with in NPI by assuming that tied observations differ by small amounts which tend to zero (Coolen, 2006). For X_{n+1}, representing a future observation, $A_{(n)}$ partially specifies a probability distribution by $P(X_{n+1} \in (x_{i-1}, x_i)) = \frac{1}{n+1}$ for $i = 1, \ldots, n+1$. $A_{(n)}$ does not assume anything else, it is a post-data assumption related to exchangeability (De Finetti, 1974). It is convenient to introduce the set of precise probability distributions which correspond to the partial specification by $A_{(n)}$, so which have probability $\frac{1}{n+1}$ in each of the $n+1$ intervals (x_{i-1}, x_i). This set is called a 'structure' by Weichselberger (2000, 2001), we denote it by $\mathcal{P}_x$.

Inferences based on $A_{(n)}$ are predictive and nonparametric, and can be considered suitable if there is hardly any knowledge about the random quantity of interest, other than the n observations, or if one does not want to use any such further information in order to derive at inferences that are strongly based on the data. The assumption $A_{(n)}$ is not sufficient to derive precise probabilities for many events of interest, but it provides bounds for probabilities via the 'fundamental theorem of probability' (De Finetti, 1974), which are lower and upper probabilities in interval probability theory (Augustin and Coolen, 2004; Walley, 1991; Weichselberger, 2000, 2001; Coolen et al., 2011).

In NPI, uncertainty about the future observation X_{n+1} is quantified by lower and upper probabilities for events of interest. Lower and upper probabilities generalize classical ('precise') probabilities. A lower (upper) probability for event A, denoted by $\underline{P}(A)$ ($\overline{P}(A)$), can be interpreted as supremum buying (infimum selling) price for a gamble on the event A (Walley, 1991), or just as the maximum lower (minimum upper) bound for the probability of A that follows from the assumptions made. This latter interpretation is used in NPI (Coolen, 2006, 2011). We wish to explore application of $A_{(n)}$ for inference without making further assumptions. So, NPI lower and upper probabilities are the sharpest bounds on a probability for an event of interest when only $A_{(n)}$ is assumed. Using the $A_{(n)}$-based structure, the NPI lower and upper probabilities for event A are

$$\underline{P}(A) = \inf_{P \in \mathcal{P}_x} P(A) \quad \text{and} \quad \overline{P}(A) = \sup_{P \in \mathcal{P}_x} P(A)$$

$\underline{P}(A)$ ($\overline{P}(A)$) can be considered to reflect the evidence in favour of (against) event A (Coolen et al., 2011). Augustin and Coolen (2004) proved that NPI has strong consistency properties in the theory of interval probability (Walley, 1991; Weichselberger, 2000, 2001; Coolen et al., 2011), it is also exactly calibrated from frequentist statistics perspective (Lawless and Fredette, 2005), which allows interpretation of the NPI lower and upper probabilities as bounds on the long-term ratio with which the event A occurs upon repeated application of this statistical procedure.

4. NPI for three-group ROC analysis

In this section, NPI for three-group ROC analysis is presented. Notation is introduced in Section 4.1, which includes the introduction of the NPI-based

structures for the next observation from each of the three groups. In Section 4.2 the lower and upper envelopes of the set of all ROC surfaces corresponding to probability distributions in these NPI-based structures are derived by pointwise optimisation. These envelopes represent this set well, but they are too wide in the sense that the volumes under their surfaces are not generally the infimum and supremum of the volumes under the ROC surfaces in this set. To define NPI lower and upper ROC surfaces such that the volumes under them are equal to this infimum and supremum, respectively, we consider the relation between the volume under an ROC surface and the probability of correctly ordered observations from the three groups. The NPI lower and upper probabilities for this event are presented in Section 4.3, with the corresponding NPI lower and upper ROC surfaces presented in Section 4.4. In Section 4.5 the choice of decision threshold for the diagnosis is considered. As computation of the NPI lower and upper ROC surfaces is not straightforward, it may be attractive to quickly derive bounds for them. The envelopes presented in Section 4.2 provide a lower bound for the NPI lower ROC surface and an upper bound for the NPI upper ROC surface. In Section 4.6 we present a quick way to derive an upper bound for the NPI lower ROC surface and a lower bound for the NPI upper ROC surface.

4.1. Notation

To develop the NPI approach for three-group ROC analysis, let X_{n_x+1}, Y_{n_y+1} and Z_{n_z+1} be the next observations from groups G_x, G_y and G_z, respectively. We apply $A_{(n)}$ for each group. Let the n_x ordered observations from group G_x be denoted by $x_1 < x_2 < \ldots < x_{n_x}$ and let $x_0 = -\infty$ and $x_{n_x+1} = \infty$ for ease of notation. For X_{n_x+1}, representing a future observation from group G_x, $A_{(n_x)}$ partially specifies a probability distribution by $P(X_{n_x+1} \in (x_{i-1}, x_i)) = \frac{1}{n_x+1}$ for $i = 1, \ldots, n_x+1$. For groups G_y and G_z the same concepts are introduced, with the obvious changes to notation. The sets of all probability distributions that correspond to these partial specifications for X_{n_x+1}, Y_{n_y+1} and Z_{n_z+1}, are the NPI-based structures and are denoted by $\mathcal{P}_x$, $\mathcal{P}_y$ and $\mathcal{P}_z$, respectively. For $x \in [x_{i-1}, x_i)$ the NPI lower CDF for X_{n_x+1} is $\underline{F}_x(x) = \frac{i-1}{n_x+1}$, $i = 1, \ldots, n_x+1$, and for $x \in (x_{i-1}, x_i]$ the NPI upper CDF for X_{n_x+1} is $\overline{F}_x(x) = \frac{i}{n_x+1}$, $i = 1, \ldots, n_x+1$. Note that there is no imprecision at the x_i, as $\underline{F}_x(x_i) = \overline{F}_x(x_i) = \frac{i}{n_x+1}$ for $i = 0, 1, \ldots, n_x+1$. These lower and upper CDFs are derived as the pointwise infima and suprema over all corresponding CDFs in the structure $\mathcal{P}_x$. The NPI lower and upper CDFs for Y_{n_y+1} and Z_{n_z+1} are similarly defined.

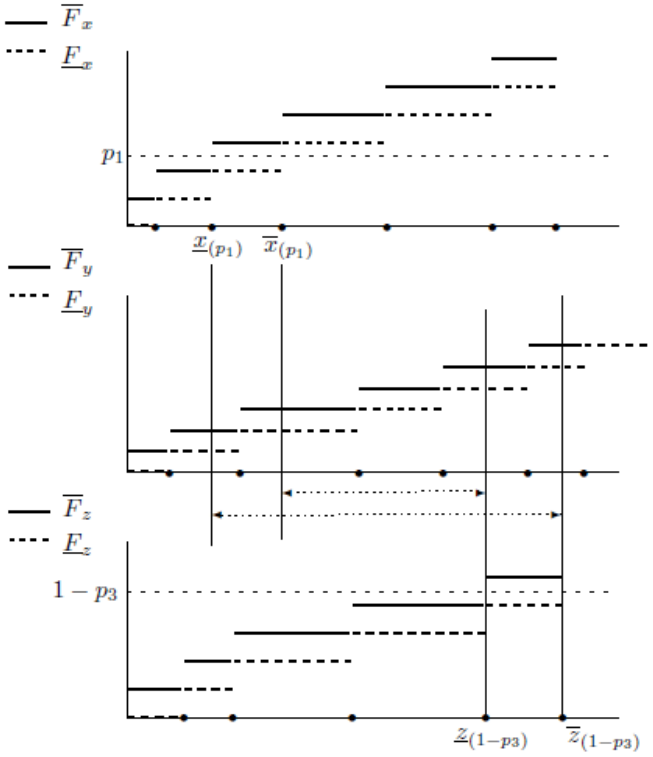

Figure 1: Construction of lower and upper envelopes of the set of NPI-based ROC surfaces

4.2. Lower and upper envelopes of the set of NPI-based ROC surfaces

For each combination of probability distributions for X_{n_x+1}, Y_{n_y+1} and Z_{n_z+1} in $\mathcal{P}_x$, $\mathcal{P}_y$ and $\mathcal{P}_z$, respectively, the corresponding ROC surface as presented in Equation (1) can be created, leading to a set of NPI-based ROC surfaces, which we denote by $\mathcal{S}_{roc}$. The lower and upper envelopes of this set, which consist of the pointwise infima and suprema, are presented in Theorem 4.1. First their construction is explained using Figure 1.

To derive the lower and upper envelopes of the set $\mathcal{S}_{roc}$, we need to derive the infima and suprema of the values $ROC_s(p_1, p_3)$ for ROC surfaces in the set $\mathcal{S}_{roc}$. Consider a value for $p_1 \in (0,1)$ that is not equal to a value $i/(n_x+1)$ for any $i \in \{1, \ldots, n_x\}$. There is a unique $i \in \{1, \ldots, n_x+1\}$ such that $x_{i-1} < F_x^{-1}(p_1) < x_i$ for every CDF F_x corresponding to all probability distributions in $\mathcal{P}_x$. As indicated in Figure 1, we denote these x_{i-1} and x_i by $\underline{x}_{(p_1)}$ and

$\overline{x}_{(p_1)}$, respectively, so $\underline{F}_x(\underline{x}_{(p_1)}) < p_1 < \overline{F}_x(\overline{x}_{(p_1)})$ for the CDFs corresponding to all probability distributions in $\mathcal{P}_x$. For $p_1 = \frac{i}{n_x+1}$, for any $i \in \{1, \ldots, n_x\}$, we would have $x_{i-1} < F_x^{-1}(p_1) < x_{i+1}$, for ease of presentation we neglect this as it only describes the envelopes at a finite number of observations. For the volumes under these lower and upper envelopes of all the ROC surfaces in $\mathcal{S}_{roc}$, which we consider later, it is also irrelevant what happens at this finite number of points. Similarly, consider a value $p_3 \in (0, 1)$ which is not equal to a value $l/(n_z + 1)$ for any $l \in \{1, \ldots, n_z\}$. We now consider all the inverse CDFs F_z^{-1}, corresponding to all probability distributions in $\mathcal{P}_z$, and we are interested in their value at $1 - p_3$. There are two consecutive observations, which we denote by $\underline{z}_{(1-p_3)}$ and $\overline{z}_{(1-p_3)}$, with $\underline{z}_{(1-p_3)} < F_z^{-1}(1 - p_3) < \overline{z}_{(1-p_3)}$ and therefore $\underline{F}_z(\underline{z}_{(1-p_3)}) < 1 - p_3 < \overline{F}_z(\overline{z}_{(1-p_3)})$. We can again neglect values of p_3 such that $1 - p_3 = \frac{l}{n_z+1}$ for any $l \in \{1, \ldots, n_z\}$, for which $z_{l-1} < F_z^{-1}(1 - p_3) < z_{l+1}$.

For any (p_1, p_3) as described above, the infimum of the values $ROC_s(p_1, p_3)$, as given by Equation (1), for all ROC surfaces in the set $\mathcal{S}_{roc}$, can be derived as follows (see Figure 1). We must find the infimum for the NPI-based probability for the event $Y_{n_y+1} \in (\overline{x}_{(p_1)}, \underline{z}_{(1-p_3)})$, this interval corresponding to the inverse CDFs is as small as possible. This is achieved by counting the number of intervals (y_{j-1}, y_j) that are totally included in $(\overline{x}_{(p_1)}, \underline{z}_{(1-p_3)})$. We denote the resulting lower envelope at the point (p_1, p_3) by $\underline{ROC}_s^L(p_1, p_3)$, it is presented in Theorem 4.1. To derive the upper envelope, the interval corresponding to the inverse CDFs is taken as large as possible, $(\underline{x}_{(p_1)}, \overline{z}_{(1-p_3)})$, and the NPI upper probability for the event that Y_{n_y+1} will be in this interval is calculated by counting the number of intervals (y_{j-1}, y_j) that have non-empty intersection with $(\underline{x}_{(p_1)}, \overline{z}_{(1-p_3)})$. We denote the resulting upper envelope at the point (p_1, p_3) by $\overline{ROC}_s^U(p_1, p_3)$, it is also presented in Theorem 4.1. No formal proof of this theorem is included, the steps follow the explanation just given, the theorem applies formally to the values of (p_1, p_3) as described above.

Theorem 4.1. The lower envelope of all NPI-based ROC surfaces in $\mathcal{S}_{roc}$ is

$$\underline{ROC}_s^L(p_1, p_3) = \begin{cases} \underline{F}_y(\underline{z}_{(1-p_3)}) - \overline{F}_y(\overline{x}_{(p_1)}) & \text{if } \underline{F}_y(\underline{z}_{(1-p_3)}) \geq \overline{F}_y(\overline{x}_{(p_1)}) \\ 0 & \text{otherwise} \end{cases} \tag{5}$$

The upper envelope of all NPI-based ROC surfaces in $\mathcal{S}_{roc}$ is

$$\overline{ROC}_s^U(p_1,p_3) = \begin{cases} \overline{F}_y(\overline{z}_{(1-p_3)}) - \underline{F}_y(\underline{x}_{(p_1)}) & \text{if } \underline{x}_{(p_1)} \leq \overline{z}_{(1-p_3)} \\ 0 & \text{otherwise} \end{cases} \tag{6}$$

It is interesting to consider the volumes under these lower and upper envelopes, which we denote by $\underline{VUS}^L$ and $\overline{VUS}^U$, respectively. These are given in Theorem 4.2, see Appendix A for the proofs.

Theorem 4.2. The volumes under the lower and upper envelopes of all NPI-based ROC surfaces in $\mathcal{S}_{roc}$ are

$$\underline{VUS}^L = A \sum_{i=1}^{n_x+1} \sum_{j=1}^{n_y+1} \sum_{l=1}^{n_z+1} I(x_i < y_{j-1} \wedge y_j < z_{l-1}) \tag{7}$$

$$\overline{VUS}^U = A \sum_{i=1}^{n_x+1} \sum_{j=1}^{n_y+1} \sum_{l=1}^{n_z+1} I(x_{i-1} < y_j \wedge x_{i-1} < z_l \wedge y_{j-1} < z_l) \tag{8}$$

where $A = \frac{1}{(n_x+1)(n_y+1)(n_z+1)}$.

These lower and upper envelopes of all NPI-based ROC surfaces in $\mathcal{S}_{roc}$ are themselves not elements of $\mathcal{S}_{roc}$. The minimisation performed to find the lower envelope at (p_1, p_3) involves putting the minimum possible NPI-based probability mass for Y_{n_y+1} in the interval $(\overline{x}_{(p_1)}, \underline{z}_{(1-p_3)})$. This pointwise optimisation gives, for all such points (p_1, p_3), solutions that cannot be obtained simultaneously, particularly because it always minimizes probability mass for Y_{n_y+1} and hence, when all the solutions are taken together, not a total probability of 1 is used for Y_{n_y+1}. With regard to X_{n_x+1} and Z_{n_z+1} this problem does not occur, as all optimisations with regard to the probability distributions for these random quantities have solutions that can be obtained simultaneously by either putting all probability masses to the left-end points or all to the right-end points of their intervals. These envelopes adequately describe the whole set of all NPI-based ROC surfaces in $\mathcal{S}_{roc}$, but are in some sense too wide as the volumes under them, $\underline{VUS}^L$ and $\overline{VUS}^U$, are not

generally equal to the infimum and supremum of the volumes under all the NPI-based ROC surfaces in $\mathcal{S}_{roc}$.

We wish to identify ROC surfaces corresponding to $\mathcal{S}_{roc}$ such that their VUS values are equal to the infimum and supremum of the VUS values for all the ROC surfaces in $\mathcal{S}_{roc}$. We present this in Section 4.4, by focusing on the volumes under the ROC surfaces and their relations to NPI lower and upper probabilities for correctly ordered observations, so for the event $X_{n_x+1} < Y_{n_y+1} < Z_{n_z+1}$. However, as the NPI lower and upper probabilities for such correctly ordered observations have not yet been presented in the literature, they are first derived in Section 4.3.

4.3. NPI lower and upper probabilities for the event $X_{n_x+1} < Y_{n_y+1} < Z_{n_z+1}$

We present the NPI lower and upper probabilities for the event $X_{n_x+1} < Y_{n_y+1} < Z_{n_z+1}$, with notation as introduced in Section 4.1. These NPI lower and upper probabilities for a specific ordering of three such future observations have not yet been presented in the literature and can be applied to a variety of problems beyond their use in Section 4.4. They are not expressable in closed form, but are derived as follows.

Theorem 4.3. The NPI lower and upper probabilities for the event $X_{n_x+1} < Y_{n_y+1} < Z_{n_z+1}$ are

$$\underline{P}(X_{n_x+1} < Y_{n_y+1} < Z_{n_z+1}) = A \sum_{i=1}^{n_x+1} \sum_{j=1}^{n_y+1} \sum_{l=1}^{n_z+1} I(x_i < t^j_{\min} < z_{l-1}) \qquad (9)$$

$$\overline{P}(X_{n_x+1} < Y_{n_y+1} < Z_{n_z+1}) = A \sum_{i=1}^{n_x+1} \sum_{j=1}^{n_y+1} \sum_{l=1}^{n_z+1} I(x_{i-1} < t^j_{\max} < z_l) \qquad (10)$$

where $A = \frac{1}{(n_x+1)(n_y+1)(n_z+1)}$ and $t^j_{\min}$ ($t^j_{\max}$) is any value belonging to a sub-interval of (y_{j-1}, y_j), for $j = 1, \ldots, n_y+1$, where the sub-intervals are created by the observations from groups G_x and G_z within this interval (y_{j-1}, y_j), such that the probability for the event $X_{n_x+1} < Y_{n_y+1} < Z_{n_z+1}$ is minimal (maximal).

These NPI lower and upper probabilities are the infimum and supremum, respectively, over all precise probabilities for this event, corresponding to

precise probability distributions for X_{n_x+1} in $\mathcal{P}_x$, Y_{n_y+1} in $\mathcal{P}_y$ and Z_{n_z+1} in $\mathcal{P}_z$. The proof of this theorem, given in Appendix B, contains explanation of the remaining optimisations required to derive these NPI lower and upper probabilities, so to determine $t^j_{\min}$ and $t^j_{\max}$.

In the following section we define NPI lower and upper ROC surfaces, for which we introduce some further notation. Let F_y^* and F_y^{**} denote the CDFs of the probability distributions created in the optimisation procedure in the proof of Theorem 4.3, as presented in Appendix B. These CDFs are step-function with probability $1/(n_y+1)$ at the values $t^j_{\min}$ and $t^j_{\max}$, respectively, for $j = 1, \ldots, n_y + 1$.

4.4. NPI lower and upper ROC surfaces

In Section 4.2 we presented the lower and upper envelopes of the set $\mathcal{S}_{roc}$ of all ROC surfaces created by combining probability distributions for X_{n_x+1}, Y_{n_y+1} and Z_{n_z+1} in the respective NPI-based structures $\mathcal{P}_x$, $\mathcal{P}_y$ and $\mathcal{P}_z$. However, as these lower and upper envelopes result from pointwise optimisation they are too wide with regard to the set $\mathcal{S}_{roc}$ when the VUS values are considered. These envelopes are of interest, e.g. to graphically present the set $\mathcal{S}_{roc}$, as will be done in the example in Section 5. But it is also important to identify surfaces that provide tight bounds to the VUS values for all ROC surfaces in the set $\mathcal{S}_{roc}$, as these values play an important role for summarizing the quality of the diagnostic test and for interpreting the ROC surfaces. Next we define ROC surfaces with VUS values equal to the infimum and supremum of the VUS values for all ROC surfaces in $\mathcal{S}_{roc}$. The equality of the VUS and the probability of correctly ordered observations enables us to define lower and upper ROC surfaces in line with the optimisation procedures in Section 4.3, we call these the NPI lower and upper ROC surfaces.

Definition 4.1. The NPI lower ROC surface is defined by, for $p_1, p_3 \in [0,1]$,

$$\underline{ROC}_s(p_1,p_3) = \begin{cases} F_y^*(\underline{z}_{(1-p_3)}) - F_y^*(\overline{x}_{(p_1)}) & \text{if } F_y^*(\underline{z}_{(1-p_3)}) \geq F_y^*(\overline{x}_{(p_1)}) \\ 0 & \text{otherwise} \end{cases} \tag{11}$$

The NPI upper ROC surface is defined by, for $p_1, p_3 \in [0,1]$,

$$\overline{ROC}_s(p_1,p_3) = \begin{cases} F_y^{**}(\overline{z}_{(1-p_3)}) - F_y^{**}(\underline{x}_{(p_1)}) & \text{if } \underline{x}_{(p_1)} \leq \overline{z}_{(1-p_3)} \\ 0 & \text{otherwise} \end{cases} \tag{12}$$

Theorem 4.4. Let the volume under the NPI lower ROC surface $\underline{ROC}_s(p_1, p_3)$ be denoted by $\underline{VUS}$, then

$$\underline{VUS} = \underline{P}(X_{n_x+1} < Y_{n_y+1} < Z_{n_z+1})$$

Similarly, let the volume under the NPI upper ROC surface $\overline{ROC}_s(p_1, p_3)$ be denoted by $\overline{VUS}$, then

$$\overline{VUS} = \overline{P}(X_{n_x+1} < Y_{n_y+1} < Z_{n_z+1})$$

The NPI lower and upper probabilities for correctly ordered observations, on the right-hand sides of the equations in Theorem 4.4, are as presented in Theorem 4.3. Due to the fact that the NPI lower and upper ROC surfaces follow precisely the construction of the NPI lower and upper probabilities in Section 4.3, the results in Theorem 4.4 are logical. For a proof of this theorem directly from Definition 4.1 we refer to Coolen-Maturi et al. (2013).

From the construction of these NPI lower and upper ROC surfaces, it follows easily that, for all $0 \leq p_1, p_3 \leq 1$,

$$\underline{ROC}_s^L(p_1, p_3) \leq \underline{ROC}_s(p_1, p_3) \leq \widehat{ROC}_s(p_1, p_3) \leq \overline{ROC}_s(p_1, p_3) \leq \overline{ROC}_s^U(p_1, p_3) \tag{13}$$

and hence

$$\underline{VUS}^L \leq \underline{VUS} \leq \widehat{VUS} \leq \overline{VUS} \leq \overline{VUS}^U \tag{14}$$

If the data from groups G_x and G_z are fully separated, with $x_{n_x} < z_1$, and there is at least one $y_j \in (x_{n_x}, z_1)$, then the NPI lower and upper ROC surfaces introduced in Definition 4.1 are equal to the lower and upper envelopes of $\mathcal{S}_{roc}$ in Theorem 4.1, of course also the corresponding volumes under these surfaces are then equal.

4.5. The NPI-based optimal decision thresholds

The choice of the decision thresholds c_1 and c_2 is an important aspect of designing the diagnostic method for the three groups case. One method is by maximisation of Youden's index as given in Equation (4). The NPI lower and upper CDFs can be used to get the NPI lower and upper probabilities of correct classifications, which can be combined into NPI lower and upper bounds for Youden's index. These are the sharpest possible bounds for all Youden's indices corresponding to probability distributions for X_{n_x+1}, Y_{n_y+1}

and Z_{n_z+1} in their respective NPI-based structures $\mathcal{P}_x$, $\mathcal{P}_y$ and $\mathcal{P}_z$. The NPI lower bound for Youden's index is

$$\begin{aligned}\underline{J}(c_1, c_2) &= \underline{P}(X_{n_x+1} \leq c_1) + \underline{P}(c_1 < Y_{n_y+1} \leq c_2) + \underline{P}(Z_{n_z+1} > c_2) \\ &= \underline{F}_x(c_1) + \left\{\underline{F}_y(c_2) - \overline{F}_y(c_1)\right\}^+ + 1 - \overline{F}_z(c_2)\end{aligned}$$

where $\{A\}^+ = \max\{A, 0\}$, and the corresponding NPI upper bound for Youden's index is

$$\begin{aligned}\overline{J}(c_1, c_2) &= \overline{P}(X_{n_x+1} \leq c_1) + \overline{P}(c_1 < Y_{n_y+1} \leq c_2) + \overline{P}(Z_{n_z+1} > c_2) \\ &= \overline{F}_x(c_1) + \overline{F}_y(c_2) - \underline{F}_y(c_1) + 1 - \underline{F}_z(c_2)\end{aligned}$$

If c_1 and c_2 do not coincide with any data observations, then it is straightforward to show that

$$\overline{J}(c_1, c_2) = \underline{J}(c_1, c_2) + \frac{1}{n_x + 1} + \frac{2}{n_y + 1} + \frac{1}{n_z + 1} \tag{15}$$

If either or both of c_1 and c_2 are equal to some data observations, then a similar relation but with fewer terms on the right-hand side is easily derived, but this is of little practical relevance. This constant difference between the NPI upper and lower Youden's indices implies that both will be maximised at the same values of c_1 and c_2. It is further easy to show that, for all c_1 and c_2,

$$\underline{J}(c_1, c_2) \leq \hat{J}(c_1, c_2) \leq \overline{J}(c_1, c_2)$$

where $\hat{J}(c_1, c_2)$ is the empirical estimate of Youden's index, obtained by using the empirical CDFs in Equation (4). These inequalities do not imply that the empirical estimate of Youden's index is maximal for the same values of c_1 and c_2 as the NPI lower and upper Youden's indices. We expect that in many situations the maxima will be attained at the same values, in particular for large data sets due to Equation (15).

4.6. Upper (lower) bound for the NPI lower (upper) ROC surface

Obtaining the NPI lower and upper ROC surfaces, as introduced in Section 4.4, is not problematic for small data sets, but deriving the values $t^j_{\min}$ and $t^j_{\max}$ for each interval (y_{j-1}, y_j) may require much computational effort for large data sets, in particular if there is much overlap between the observations from the three groups. To avoid the numerical optimisation required

to derive the NPI lower and upper ROC surfaces, the envelopes presented in Section 4.2 can be used as approximations, these are available in simple expressions as given in Theorem 4.1. The lower envelope is a lower bound for the NPI lower ROC surface, the upper envelope is an upper bound for the NPI upper ROC surface. We now present an upper bound for the NPI lower ROC surface and a lower bound for the NPI upper ROC surface, both of which are also easy to compute. Having both a lower and upper bound for the NPI lower ROC surface as well as for the NPI upper ROC surface, without requiring numerical optimisation procedures, is useful, to get insight into the actual NPI lower and upper ROC surfaces and the corresponding VUS values.

We present these further bounds in Definition 4.2. They are derived by putting the probability masses for X_{n_x+1} and Z_{n_z+1} at the same end points per interval as for the lower and upper envelopes presented in Section 4.2, while for Y_{n_y+1} we use the probability distribution corresponding to the NPI lower CDF $\underline{F}_y$ (any probability distribution in $\mathcal{P}_y$ could be taken; for a more detailed presentation see Coolen-Maturi et al. (2013)).

Definition 4.2. An upper bound for the NPI lower ROC surface can be defined by

$$\underline{ROC}_s^U(p_1, p_3) = \begin{cases} \underline{F}_y(\underline{z}_{(1-p_3)}) - \underline{F}_y(\overline{x}_{(p_1)}) & \text{if } \underline{F}_y(\underline{z}_{(1-p_3)}) \geq \underline{F}_y(\overline{x}_{(p_1)}) \\ 0 & \text{otherwise} \end{cases} \tag{16}$$

A lower bound for the NPI upper ROC surface can be defined by

$$\overline{ROC}_s^L(p_1, p_3) = \begin{cases} \underline{F}_y(\overline{z}_{(1-p_3)}) - \underline{F}_y(\underline{x}_{(p_1)}) & \text{if } \underline{x}_{(p_1)} \leq \overline{z}_{(1-p_3)} \\ 0 & \text{otherwise} \end{cases} \tag{17}$$

The volumes under these bounding surfaces are given in Theorem 4.5. Its proof follows the same steps as the proof in Appendix A, and is presented in detail by Coolen-Maturi et al. (2013).

Theorem 4.5. The volume under the bounding surface $\underline{ROC}_s^U(p_1, p_3)$ is

$$\underline{VUS}^U = A \sum_{i=1}^{n_x+1} \sum_{j=1}^{n_y+1} \sum_{l=1}^{n_z+1} I(x_i < y_j < z_{l-1}) \tag{18}$$

and the volume under the bounding surface $\overline{ROC}_s^L(p_1, p_3)$ is

$$\overline{VUS}^L = A \sum_{i=1}^{n_x+1} \sum_{j=1}^{n_y+1} \sum_{l=1}^{n_z+1} I(x_{i-1} < y_j < z_l) \tag{19}$$

where $A = \frac{1}{(n_x+1)(n_y+1)(n_z+1)}$.

From their constructions it is easy to see that, for all $p_1, p_3 \in [0, 1]$,

$$\begin{aligned} \underline{ROC}_s^L(p_1, p_3) \le \underline{ROC}_s(p_1, p_3) \le \underline{ROC}_s^U(p_1, p_3) \\ \overline{ROC}_s^L(p_1, p_3) \le \overline{ROC}_s(p_1, p_3) \le \overline{ROC}_s^U(p_1, p_3) \\ \underline{VUS}^L \le \underline{VUS} \le \underline{VUS}^U \text{ and } \overline{VUS}^L \le \overline{VUS} \le \overline{VUS}^U \end{aligned}$$

5. Example

We illustrate the NPI approach presented in this paper via an example, using data from the literature concerning the diagnostic test NAA/Cr which is used to discriminate between different levels of HIV among patients (Chang et al., 2004; Yiannoutsos et al., 2008; Nakas et al., 2010). The data consist of observations for 135 patients, of whom 59 were HIV-positive with AIDS dementia complex (ADC), 39 were HIV-positive non-symptomatic subjects (NAS), and 37 were HIV-negative individuals (NEG) (Nakas et al., 2010; Inacio et al., 2011). The NAA/Cr levels are expected to be lowest among the ADC group and highest among the NEG group, with the NAS group being the intermediate group (Chang et al., 2004) (in relation to the presentation in this paper, these are groups G_x, G_z and G_y, respectively). Figure 2 shows the boxplots of these data, which overlap considerably, particularly the NAS and NEG groups.

The lower and upper envelopes $\underline{ROC}_s^L(p_1, p_3)$ and $\overline{ROC}_s^U(p_1, p_3)$ for the set $\mathcal{S}_{roc}$ of all NPI-based ROC surfaces are presented in Figure 3, together with the empirical ROC surface. In these plots, p_1 and p_3 increase from 0 to 1 in the directions indicated by arrows. The empirical ROC surface is everywhere between the two envelopes but the differences are small. The NPI lower and upper ROC surfaces, presented in Section 4.4, are not plotted, they are contained within the envelopes and differ only very little from them.

The VUS values of the seven surfaces presented in this paper, so also including the further bounds in Section 4.6, are given in Table 1. They reflect

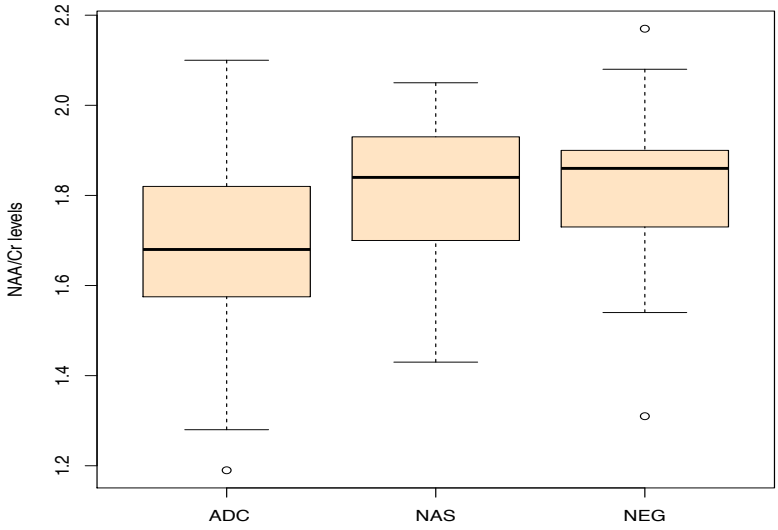

Figure 2: Boxplots of NAA/Cr levels for the ADC, NAS and NEG groups

indeed that the differences between these surfaces are small. To interpret these values, it is important to remember that a VUS of about 1/6 occurs if the observations from the three groups fully overlap, in such a way that the diagnostic method would perform no better than a random allocation of patients to the three groups. As all VUS values are clearly greater than 1/6, this indicates that the diagnostic method is better than a random allocation. However, the VUS values are far away from 1, which would indicate perfect diagnostic performance. It is clear from Figure 2 that particularly the data from the NAS and NEG groups overlap substantially. These VUS values also imply that the NPI lower and upper ROC surfaces are close to the corresponding envelopes and that the upper bound for the NPI lower ROC surface and the lower bound for the NPI upper ROC surface are a bit further from the NPI lower and upper ROC surfaces than the corresponding envelopes. All bounds together could be useful if one would not have gone through the efforts of calculating the NPI lower and upper ROC surfaces exactly, as they would provide ranges within which the exact surfaces are.

The maximum value of Youden's index corresponding to the empirical

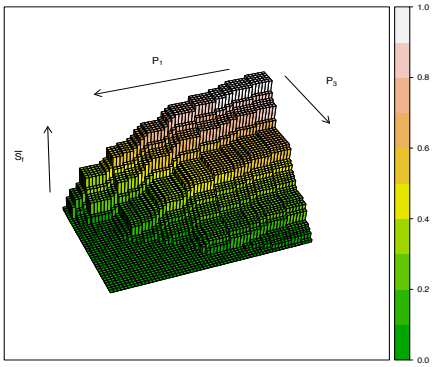

(a) Upper envelope

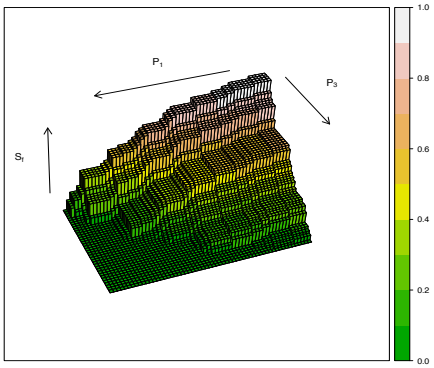

(b) Empirical ROC surface

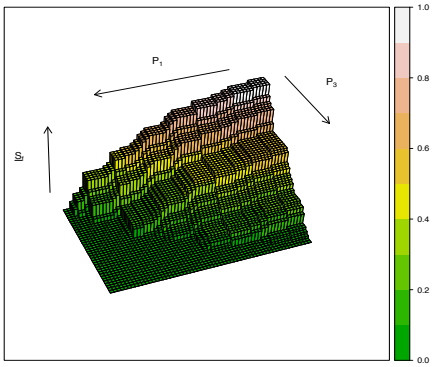

(c) Lower envelope

Figure 3: Upper and lower envelopes and empirical ROC surface

Table 1: Volumes under ROC surfaces

$\widehat{VUS}$	0.2879
$(\underline{VUS}^L, \overline{VUS}^U)$	(0.2524,0.3131)
$(\underline{VUS}, \overline{VUS})$	(0.2548,0.3087)
$(\underline{VUS}^U, \overline{VUS}^L)$	(0.2688,0.2951)

ROC surface is equal to 1.4362, which occurs for $(c_1, c_2) = (1.76, 2.05)$. The maximum values for the Youden's indices corresponding to the NPI lower and upper ROC surfaces are $\underline{J}(c_1, c_2) = 1.3803$ and $\overline{J}(c_1, c_2) = 1.4732$, which both occur for the same values of c_1 and c_2 as for the empirical ROC surface. These maximum values for the Youden's indices indicate that the diagnostic performance of this test for the next patient is likely to be better than random classification, but it is not very good. With these optimal decision thresholds for diagnosis of the next patient, a test result less than or equal to 1.76 leads to classification into the ADC group, a test result greater than 2.05 leads to classification into the NEG group, and a rest result in between these two values leads to classification into the NAS group. The corresponding NPI lower and upper probabilities for correct classification are 0.6000 and 0.6167 for the next patient if from the ADC group, 0.6750 and 0.7250 if from the NAS group, and 0.1053 and 0.1316 if from the NEG group. The substantial overlap between the data from the NAS and NEG groups has resulted in an optimal classification method where nearly the entire range of values of this overlap leads to classification in the NAS group, which explains the small values of the NPI lower and upper probabilities for correct classification if the next patient is from the NEG group.

Coolen-Maturi et al. (2013) present two further examples, with smaller data sets and with less overlap between the data from the three groups. They illustrate some further aspects of this NPI approach, including that the difference between corresponding NPI upper and lower probabilities tends to be greater if there are fewer data observations and thus reflects the amount of information on which the inferences are based. Of course, if there is less overlap between the data from the three groups, the classification methods perform substantially better than in the example presented here.

6. Concluding remarks

In this paper we introduced the NPI approach for three-group diagnostic tests using the ROC surface. This can be used to asses the accuracy of a diagnostic test, with the NPI setting ensuring, due to its predictive nature, specific focus on the next patient. NPI lower probabilities reflect the evidence in favour of the event of interest, while NPI upper probabilities reflect the evidence against the event of interest. When making decisions about diagnosis for a specific future patient, it seems useful to have the amount of information and the evidence it provides clearly reflected in this way.

Attention has been restricted to real-valued data, developing the related NPI theory for ROC surfaces in case of ordinal data is an interesting topic for future research (Elkhafifi and Coolen, 2012; Coolen et al., 2013). The concepts and ideas presented can be generalized to classification into more than three categories (Waegeman et al., 2008), but the computation of NPI lower and upper ROC hypersurfaces, in line with Section 4.4, will require numerical optimisation which will be complicated for larger data sets with substantial overlap between observations from different groups. Generalization of the lower and upper envelopes of the set of all NPI-based ROC hypersurfaces is likely to remain feasible with more categories, but it has not yet been studied in detail. Heuristic methods to approximate the NPI lower and upper ROC hypersurfaces may be required, the quality of such approximations, in relation to the computational complexity for their implementation, requires detailed study.

Development of NPI methods for ROC analysis including covariates is an important challenge (Lopez-de Ullibarri et al., 2008; Rodriguez-Alvarez et al., 2011a,b). Research of a general NPI approach for regression-type models is currently in progress. It is also possible to assume semi-parametric models in ROC analysis (Zhang, 2006; Wan and Zhang, 2008; Li and Zhou, 2009). Combining the NPI approach with partial parametric model assumptions, which would also enable application to ROC problems, is an important topic for future research. Increasingly, statistical data are high-dimensional, which sets new challenges for analysis of diagnostic accuracy including ROC methods (Adler and Lausen, 2009). NPI has not yet been developed for multi-dimensional data, it is an important research challenge and may require additional structural model assumptions due to the curse of dimensionality that generally affects nonparametric methods.

As the NPI approach does not aim at estimating characteristics for an

assumed underlying population, but instead explicitly focuses on a future observation, it is quite different in nature to the established statistical approaches, but in practice a predictive formulation may often be natural. NPI for real-valued observations is also available for multiple future observations (Arts et al., 2004; Coolen, 2011), where the inter-dependence of these future observations is explicitly taken into account. Development of NPI-based methods for diagnostic accuracy with explicit focus on $m \geq 2$ future observations is an interesting topic for future research, where particularly the strength of the inferences as function of m should be studied carefully, see Coolen and Coolen-Schrijner (2007) for a similar study with focus on the role of m for comparison of groups of Bernoulli data. Typically, for increasing m the imprecision in inferences increases, which is likely to imply that, on the basis of the limited information in available data, a specific choice of diagnostic method including the important decision thresholds can be inferred to be good for a number of future patients up to a specific value of m, but for larger values of m the evidence in the data would be too weak to make decisions that are strongly supported by the data without further modelling assumptions.

We should emphasize that we do not advocate the NPI approach presented here as a replacement of more established methods, but as an interesting alternative approach to important problems which we recommend to be used alongside other methods. If the results of different methods are quite close that provides a strong argument in favour of them, while substantial differences might suggest that further investigation would be beneficial. In particular, as most established statistical methods make stronger modelling assumptions, it would be logical in such cases to consider whether or not such assumptions are supported by the data.

There is a wide range of related topics which are of practical relevance but require further research. This includes dealing with continuous disease states which also need to be classified into groups (Shiu and Gatsonis, 2012), and the use of alternatives to the VUS (van Calster et al., 2012) or Youden's index in such ROC-based analyses (Greiner et al., 2000; Schafer, 1989; Yousef et al., 2009; Lai et al., 2012). The possibility that the data may contain errors is also of great practical importance. All such topics provide interesting challenges for the further development and application of the NPI approach.

Acknowledgement
We are grateful to Dr. Christos Nakas for stimulating discussions about this topic area and for providing the data used in the example. We thank two reviewers whose detailed comments on an earlier version of this paper led to improved presentation.

Appendix A

In this paper, several volumes under surfaces have been presented. They are all proven following similar steps, which we present for Equation (7); they are all presented in detail by Coolen-Maturi et al. (2013). We use the notation $\{A\}^+ = \max\{A, 0\}$ and $\sum_{p_1}\sum_{p_3}$ to indicate the sum over pairs of values for p_1 and p_3 such that one value for p_1 is taken from each interval $(\frac{i-1}{n_x+1}, \frac{i}{n_x+1})$ for $i = 1, \ldots, n_x + 1$, and one value for p_3 from each interval $(\frac{l-1}{n_z+1}, \frac{l}{n_z+1})$ for $l = 1, \ldots, n_z + 1$. As the considered ROC surfaces are constant for all values $p_1 \in (\frac{i-1}{n_x+1}, \frac{i}{n_x+1})$ and $p_3 \in (\frac{l-1}{n_z+1}, \frac{l}{n_z+1})$, it does not matter which specific values for p_1 and p_3 within these intervals are actually used in the calculations (e.g. mid-points of the intervals). Equation (7) is derived as follows.

$$\begin{aligned}
\underline{VUS}^L &= \frac{1}{(n_x+1)(n_z+1)} \sum_{p_1}\sum_{p_3} \underline{ROC}_s^L(p_1, p_3) \\
&= \frac{1}{(n_x+1)(n_z+1)} \sum_{p_1}\sum_{p_3} \left\{\underline{F}_y(\underline{z}_{(1-p_3)}) - \overline{F}_y(\overline{x}_{(p_1)})\right\}^+ \\
&= \frac{1}{(n_x+1)(n_z+1)} \sum_{i=1}^{n_x+1}\sum_{l=1}^{n_z+1} \left\{\underline{F}_y(z_{l-1}) - \overline{F}_y(x_i)\right\}^+ \\
&= A \sum_{i=1}^{n_x+1}\sum_{l=1}^{n_z+1} \left\{\sum_{j=1}^{n_y+1} I(y_j \leq z_{l-1}) - \sum_{j=1}^{n_y+1} I(y_{j-1} \leq x_i)\right\}^+ \\
&= A \sum_{i=1}^{n_x+1}\sum_{j=1}^{n_y+1}\sum_{l=1}^{n_z+1} I\left(y_j \leq z_{l-1} \wedge y_{j-1} > x_i\right)
\end{aligned}$$

Appendix B

We present a proof for Theorem 4.3. For known probability distributions for the random quantities X_{n_x+1}, Y_{n_y+1} and Z_{n_z+1},

$$P(X_{n_x+1} < Y_{n_y+1} < Z_{n_z+1})$$
$$= \sum_{i=1}^{n_x+1} \sum_{j=1}^{n_y+1} \sum_{l=1}^{n_z+1} P\left\{X_{n_x+1} < Y_{n_y+1} < Z_{n_z+1} | X_{n_x+1} \in (x_{i-1}, x_i), Y_{n_y+1} \in (y_{j-1}, y_j)\right.,$$
$$\left. Z_{n_z+1} \in (z_{l-1}, z_l)\right\} \times P(X_{n_x+1} \in (x_{i-1}, x_i)) P(Y_{n_y+1} \in (y_{j-1}, y_j)) P(Z_{n_z+1} \in (z_{l-1}, z_l))$$

This holds for all combinations of probability distributions for X_{n_x+1} in $\mathcal{P}_x$, Y_{n_y+1} in $\mathcal{P}_y$ and Z_{n_z+1} in $\mathcal{P}_z$. We need to find the infimum and supremum for this probability over all these combinations.

To derive the NPI lower probability for this event, the probability $1/(n_x+1)$ for X_{n_x+1}, as assigned to each interval in the partition of the real-line created by the observations from group G_x, is put at the right-end point of each interval. Simultaneously, the probability $1/(n_z+1)$ for Z_{n_z+1}, as assigned to each interval in the partition of the real-line created by the observations from group G_z, is put at the left-end point of each interval. This leads to

$$\inf_{\mathcal{P}_x, \mathcal{P}_y, \mathcal{P}_z} P(X_{n_x+1} < Y_{n_y+1} < Z_{n_z+1}) = \frac{1}{(n_x+1)(n_z+1)} \times$$
$$\inf_{\mathcal{P}_y} \sum_{i=1}^{n_x+1} \sum_{j=1}^{n_y+1} \sum_{l=1}^{n_z+1} P(x_i < Y_{n_y+1} < z_{l-1} | Y_{n_y+1} \in (y_{j-1}, y_j)) P(Y_{n_y+1} \in (y_{j-1}, y_j)) \tag{20}$$

Here the infima are with regard to all probability distributions in the respective structures.

By similar reasoning, the corresponding NPI upper probability requires the probability masses for X_{n_x+1} and Z_{n_z+1} to be put at the opposite end points of the respective intervals. This leads to

$$\sup_{\mathcal{P}_x, \mathcal{P}_y, \mathcal{P}_z} P(X_{n_x+1} < Y_{n_y+1} < Z_{n_z+1}) = \frac{1}{(n_x+1)(n_z+1)} \times$$
$$\sup_{\mathcal{P}_y} \sum_{i=1}^{n_x+1} \sum_{j=1}^{n_y+1} \sum_{l=1}^{n_z+1} P(x_{i-1} < Y_{n_y+1} < z_l | Y_{n_y+1} \in (y_{j-1}, y_j)) P(Y_{n_y+1} \in (y_{j-1}, y_j)) \tag{21}$$

The remaining optimisation problems are how to assign the probability masses $1/(n_y+1)$ for Y_{n_y+1} within each interval (y_{j-1}, y_j), $j = 1, \ldots, n_y+1$, for the NPI lower probability and for the NPI upper probability. Let the number of observations from groups G_x and G_z between y_{j-1} and y_j be denoted by n_x^j and n_z^j, respectively. These observations partition the interval (y_{j-1}, y_j) into $n_x^j + n_z^j + 1$ sub-intervals, the assumption that the data contain no ties simplifies notation but can be relaxed without affecting the approach. If there are no observations from groups G_x and G_z in the interval (y_{j-1}, y_j), then the following reasoning still applies with this whole interval being the only 'sub-interval'.

It is easy to see that this optimisation with regard to the probability distribution for Y_{n_y+1} can be achieved by putting the probability mass $1/(n_y+1)$ within an interval (y_{j-1}, y_j) in a single point, say t_{mi}^j related to the infimum and t_{ma}^j related to the supremum. Doing this for all $j = 1, \ldots, n_y+1$, and using the NPI lower and upper CDFs for X_{n_x+1} and Z_{n_z+1}, the optimisation problem (20) is equivalent to

$$\inf \frac{1}{n_y+1} \sum_{j=1}^{n_y+1} \underline{F}_x(t_{mi}^j)(1 - \overline{F}_z(t_{mi}^j))$$

and the optimisation problem (21) is equivalent to

$$\sup \frac{1}{n_y+1} \sum_{j=1}^{n_y+1} \overline{F}_x(t_{ma}^j)(1 - \underline{F}_z(t_{ma}^j))$$

where the infimum and supremum are with regard to the values t_{mi}^j and t_{ma}^j over all possible sub-intervals of (y_{j-1}, y_j) for each $j \in \{1, \ldots, n_y+1\}$. These optimisations can be solved by minimising and maximising, respectively, the products within the sums on the right-hand sides. As these lower and upper CDFs are step-functions, these optimisations can be quite easily performed. However, these products are not monotone over the intervals (y_{j-1}, y_j), so careful searches are required. This can be simplified using the knowledge that the CDFs are non-decreasing step-functions, and the fact that it is irrelevant which specific point within a sub-interval (as created by the x and z observations) is chosen. It is quite straightforward to implement an algorithm for these optimisations, one can take e.g. the mid-point of each sub-interval as candidate point to be t_{mi}^j or t_{ma}^j.

Once these optimisations have been performed, we denote the points to which the probability masses for Y_{n_y+1} in the intervals (y_{j-1}, y_j) are assigned by $t^j_{\min}$ and $t^j_{\max}$, $j = 1, \ldots, n_y + 1$, these are the points used in Theorem 4.3.

References

Adler, W., Lausen, B., 2009. Bootstrap estimated true and false positive rates and ROC curve. Computational Statistics & Data Analysis 53, 718–729.

Airola, A., Pahikkala, T., Waegeman, W., De Baets, B., Salakoski, T., 2011. An experimental comparison of cross-validation techniques for estimating the area under the ROC curve. Computational Statistics & Data Analysis 55, 1828–1844.

Arts, G.R.J., Coolen, F.P.A., van der Laan, P., 2004. Nonparametric predictive inference in statistical process control. Quality Technology and Quantitative Management 1, 201–216.

Augustin, T., Coolen, F.P.A., 2004. Nonparametric predictive inference and interval probability. Journal of Statistical Planning and Inference 124, 251–272.

Beck, A.C., 2005. Receiver Operating Characteristic surfaces: Inference and Applications. Ph.D. thesis. University of Rochester. Rochester, New York.

van Calster, B., van Belle, V., Vergouwe, Y., Steyerberg, E.W., 2012. Discrimination ability of prediction models for ordinal outcomes: Relationships between existing measures and a new measure. Biometrical Journal 54, 674–685.

Chang, L., Lee, P.L., Yiannoutsos, C.T., Ernst, T., Marra, C.M., Richards, T., Kolson, D., Schifitto, G., Jarvik, J.G., Miller, E.N., Lenkinski, R., Gonzalez, G., Navia, B.A., 2004. A multicenter in vivo proton-mrs study of hiv-associated dementia and its relationship to age. NeuroImage 23, 1336–1347.

Chen, W., Yousef, W., Gallas, B., Hsu, E., Lababidi, S., Tang, R., Pennello, G., Symmans, W., Pusztai, L., 2012. Uncertainty estimation with a finite dataset in the assessment of classification models. Computational Statistics & Data Analysis 56, 1016–1027.

Coolen, F.P.A., 2006. On nonparametric predictive inference and objective bayesianism. Journal of Logic, Language and Information 15, 21–47.

Coolen, F.P.A., 2011. Nonparametric predictive inference, in: Lovric, M. (Ed.), International Encyclopedia of Statistical Science. Springer, pp. 968–970.

Coolen, F.P.A., Coolen-Schrijner, P., 2007. Nonparametric predictive comparison of proportions. Journal of Statistical Planning and Inference 137, 23–33.

Coolen, F.P.A., Coolen-Schrijner, P., Coolen-Maturi, T., Elkhafifi, F.F., 2013. Nonparametric predictive inference for ordinal data. Communications in Statistics - Theory and Methods to appear.

Coolen, F.P.A., Troffaes, M.C., Augustin, T., 2011. Imprecise probability, in: Lovric, M. (Ed.), International Encyclopedia of Statistical Science. Springer, pp. 645–648.

Coolen-Maturi, T., Coolen-Schrijner, P., Coolen, F.P.A., 2012a. Nonparametric predictive inference for binary diagnostic tests. Journal of Statistical Theory and Practice 6, 665–680.

Coolen-Maturi, T., Coolen-Schrijner, P., Coolen, F.P.A., 2012b. Nonparametric predictive inference for diagnostic accuracy. Journal of Statistical Planning and Inference 142, 1141–1150.

Coolen-Maturi, T., Elkhafifi, F.F., Coolen, F.P.A., 2013. Nonparametric predictive inference for three-group ROC analysis. Technical Report (www.npi-statistics.com).

De Finetti, B., 1974. Theory of Probability. Wiley, London.

Elkhafifi, F.F., Coolen, F.P.A., 2012. Nonparametric predictive inference for accuracy of ordinal diagnostic tests. Journal of Statistical Theory and Practice 6, 681–697.

Greiner, M., Pfeiffer, D., Smith, R.D., 2000. Principles and practical application of the receiver-operating characteristic analysis for diagnostic tests. Preventive Veterinary Medicine 45, 23–41.

Heckerling, P.S., 2001. Parametric three-way receiver operating characteristic surface analyis using Mathematica. Medical Decision Making 20, 409–417.

Hill, B.M., 1968. Posterior distribution of percentiles: Bayes' theorem for sampling from a population. Journal of the American Statistical Association 63, 677–691.

Inacio, V., Turkman, A.A., Nakas, C.T., Alonzo, T.A., 2011. Nonparametric Bayesian estimation of the the three-way receiver operating characteristic surface. Biometrical Journal 53, 1011–1024.

Lai, C., Tian, L., Schisterman, E., 2012. Exact confidence interval estimation for the youden index and its corresponding optimal cut-point. Computational Statistics & Data Analysis 56, 1103–1114.

Lawless, J.F., Fredette, M., 2005. Frequentist prediction intervals and predictive distributions. Biometrika 92, 529–542.

Li, J., Zhou, X.H., 2009. Nonparametric and semiparametric estimation of the three way receiver operating characteristic surface. Journal of Statistical Planning and Inference 139, 4133–4142.

Lopez-de Ullibarri, I., Cao, R., Cadarso-Suarez, C., Lado, M., 2008. Nonparametric estimation of conditional ROC curves: Application to discrimination tasks in computerized detection of early breast cancer. Computational Statistics & Data Analysis 52, 2623–2631.

Mossman, D., 1999. Three-way rocs. Medical Decision Making 19, 78–89.

Nakas, C.T., Alonzo, T.A., 2007. ROC graphs for assessing the ability of a diagnostic marker to detect three disease classes with an umbrella ordering. Biometrics 63, 603–609.

Nakas, C.T., Alonzo, T.A., Yiannoutsos, C.T., 2010. Accuracy and cut-off point selection in three-class classification problems using a generalization of the youden index. Statistics in Medicine 29, 2946–2955.

Nakas, C.T., Yiannoutsos, C.T., 2004. Ordered multiple-class ROC analysis with continuous measurements. Statistics in Medicine 23, 3437–3449.

Nakas, C.T., Yiannoutsos, C.T., 2010. Ordered multiple class receiver operating characteristic (ROC) analysis, in: Chow, S.C. (Ed.), Encyclopedia of Biopharmaceutical Statistics. Informa Healthcare, pp. 929–932.

Pepe, M.S., 2003. The Statistical Evaluation of Medical Tests for Classification and Prediction. Oxford University Press, Oxford.

Rodriguez-Alvarez, M., Roca-Pardinas, J., Cadarso-Suarez, C., 2011a. A new flexible direct ROC regression model: Application to the detection of cardiovascular risk factors by anthropometric measures. Computational Statistics & Data Analysis 55, 3257–3270.

Rodriguez-Alvarez, M., Tahoces, P., Cadarso-Suarez, C., Lado, M., 2011b. Comparative study of ROC regression techniques - applications for the computer-aided diagnostic system in breast cancer detection. Computational Statistics & Data Analysis 55, 888–902.

Schafer, H., 1989. Constructing a cut-off point for a quantitative diagnostic test. Statistics in Medicine 8, 1381–1391.

Shiu, S.Y., Gatsonis, C., 2012. On ROC analysis with nonbinary reference standard. Biometrical Journal 54, 457–480.

Tian, L., Xiong, C., Lai, Y., Vexler, A., 2011. Exact confidence interval estimation for the difference in diagnostic accuracy with three ordinal diagnostic groups. Journal of Statistical Planning and Inference 141, 549–558.

Waegeman, W., De Baets, B., Boullart, L., 2008. On the scalability of ordered multi-class ROC analysis. Computational Statistics & Data Analysis 52, 3371–3388.

Walley, P., 1991. Statistical Reasoning with Imprecise Probabilities. Chapman & Hall, London.

Wan, S., Zhang, B., 2008. Comparing correlated ROC curves for continuous diagnostic tests under density ratio models. Computational Statistics & Data Analysis 52, 233–245.

Weichselberger, K., 2000. The theory of interval-probability as a unifying concept for uncertainty. International Journal of Approximate Reasoning 24, 149–170.

Weichselberger, K., 2001. Elementare Grundbegriffe einer allgemeineren Wahrscheinlichkeitsrechnung I. Intervallwahrscheinlichkeit als umfassendes Konzept. Physica, Heidelberg.

Wians, F.H.J., Urban, J.E., Keffer, J.H., Kroft, S.H., 2001. Discriminating between iron deficiency anemia and anemia of chronic disease using traditional indices of iron status vs transferrin receptor concentration. American Journal of Clinical Pathology 115, 112–118.

Xanthopoulos, S.Z., Nakas, C.T., 2007. A generalized ROC approach for the validation of credit rating systems and scorecards. The Journal of Risk Finance 8, 481 – 488.

Xiong, C., van Belle, G., Miller, J.P., Yan, Y., Gao, F., Yu, K., Morris, J.C., 2007. A parametric comparison of diagnostic accuracy with three ordinal diagnostic groups. Biometrical Journal 49, 682–693.

Yiannoutsos, C.T., Nakas, C.T., Navia, B.A., 2008. Assessing multiple-group diagnostic problems with multi-dimensional receiver operating characteristic surfaces: Application to proton mr spectroscopy (mrs) in hiv-related neurological injury. Neuroimage 40, 248–255.

Youden, W.J., 1950. Index for rating diagnostic tests. Cancer 3, 32–35.

Yousef, W., Kundu, S., Wagner, R., 2009. Nonparametric estimation of the threshold at an operating point on the ROC curve. Computational Statistics & Data Analysis 53, 4370–4383.

Zhang, B., 2006. A semiparametric hypothesis testing procedure for the ROC curve area under a density ratio model. Computational Statistics & Data Analysis 50, 1855–1876.

Zhou, X.H., Obuchowski, N.A., McClish, D.K., 2011. Statistical Methods in Diagnostic Medicine. Wiley, New York.

Zou, K.H., Liu, A., Bandos, A.I., Ohno-Machado, L., Rockette, H.E., 2011. Statistical Evaluation of Diagnostic Performance: Topics in ROC Analysis. Chapman Hall / CRC, Boca Raton.